New superconductors under very high pressure

2007 J. Phys.: Condens. Matter 19 125207

(http://iopscience.iop.org/0953-8984/19/12/125207)

IOP PUBLISHING JOURNAL OF PHYSICS: CONDENSED MATTER

J. Phys.: Condens. Matter **19** (2007) 125207 (11pp) doi:10.1088/0953-8984/19/12/125207

New superconductors under very high pressure

Katsuya Shimizu

KYOKUGEN, Center for Quantum Science and Technology under Extreme Conditions, Osaka University, 1-3, Machikaneyama, Toyonaka, Osaka 560-8531, Japan

E-mail: shimizu@cqst.osaka-u.ac.jp

Received 3 January 2007
Published 6 March 2007
Online at stacks.iop.org/JPhysCM/19/125207

Abstract

We have developed extreme conditions combining very low temperature and very high pressure of down to 30 mK and up to 200 GPa, respectively. These conditions are realized by using a DAC (diamond-anvil cell) which we designed for assembly on a powerful ^{3}He/^{4}He dilution refrigerator. Using these apparatus and techniques, we have searched for pressure-induced superconductivity in various materials, especially in elements under pressure. Here our experimental techniques and experimental results are reviewed.

1. Introduction

The popular diamond-anvil cell (DAC) is the most powerful piece of equipment for generating static pressure. We have newly constructed a compact and nonmagnetic DAC especially for low-temperature research. Combination with refrigerators has made it possible to study condensed matter physics in an unprecedentedly wide pressure–temperature range. One of the most aggressive challenges at high pressure is to search for, or to realize, 'metallic hydrogen', which is predicted [1] to show room-temperature superconductivity. Metallic hydrogen has long fascinated high-pressure physicists. Nobody has been able to see it in the laboratory, however it is believed to exist in fact in the interior of giant planets such as Jupiter and Saturn. Another challenge is the topic of 'superconductivity' and 'magnetism'. It is well known that ferromagnetic metals do not show superconductivity, and even a small amount of magnetic impurities can suppress the superconductivity. We can expect the appearance of superconductivity in the high-pressure phase even from magnetic metals. In the case of iron, the superconducting transition temperature was theoretically predicted to be 0.25 K [2], which is our most motivating force to carry out these studies.

2. Experimental detail

In this section, our developments and their experimental details are described. Secondly, examples of new superconductors at very high pressure are shown.

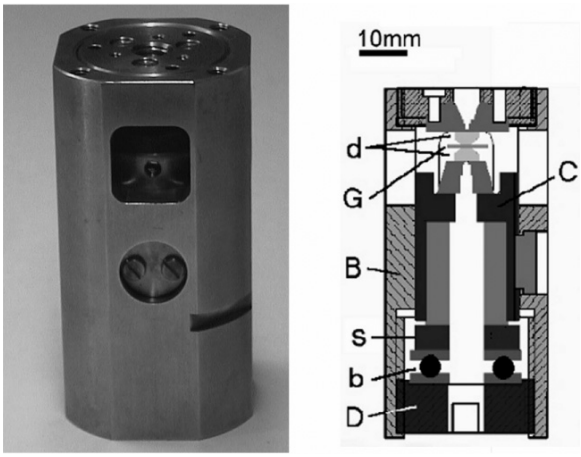

Figure 1. Photograph (left) and schematic drawing (right) of the DAC: B, main bod; C, piston with lower diamond; D, loading nut; G, gasket; b, ball bearing; d, diamond; s, plastic ring.

2.1. Pressure cell

Electrical transport measurements in a DAC can provide both proof of metalization and superconductivity at low temperature. However, in general, electrical measurements are difficult using a DAC, especially at megabar pressures, because of the problem of wiring to the small sample and insulation between the electrical wires and the metal gasket. We solved these problems and succeeded in performing four-probe electrical resistance measurements in a DAC at a pressure of 200 GPa. Using these experimental techniques, we have concentrated on searching for metallization and superconductivity in simple systems such as elements like halogen, chalcogen, 3d-magnetic metals, and alkaline metals. For the purpose of searching for pressure-induced superconductivity at low temperature, we have employed good thermally conducting materials for all parts of the DAC and performed electrical resistance measurements and/or sensitive magnetization measurements.

The DAC was also required to be nonmagnetic at low temperature to avoid the suppression of superconductivity by the magnetic field from the magnetic parts used in the DAC. The nonmagnetic pressure cell is also useful for experiments under an external magnetic field. The construction of the DAC is shown in figure 1. The main body of the cell, except for the pair of diamond-anvil and bearings, was made of a Cu–Be alloy which has relatively good thermal conductivity and low magnetization even at low temperatures below 1 K. Pressure was generated by rotating the nut with a gearbox assembly.

2.2. Applying pressure and combination with low-temperature measurements

We usually generated and clamped the pressure at room temperature before low-temperature runs. After the generation of pressure, the DAC was fixed on the mixing chamber of the ^{3}He/^{4}He dilution refrigerator. In order to be inserted into our superconducting magnet bore size, the DAC was small (less than 35 mm in diameter). Because of the difference in the magnitudes of thermal expansion between Be–Cu and diamond, pressure usually increased during cooling with our clamp-type DAC, sometimes damaging the diamonds at low temperature. In order to reduce the pressure change, we inserted a plastic ring between the piston and the nut, and then succeeded in keeping the pressure within several per cent even at

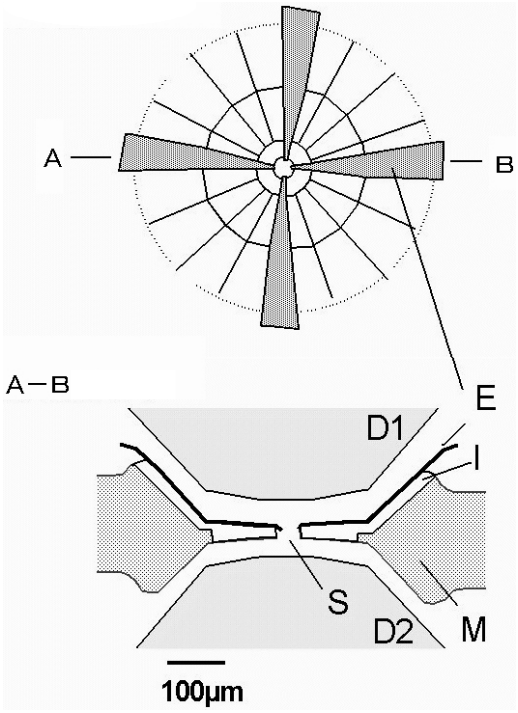

Figure 2. Schematic of probe arrangements for megabar resistance measurement in DAC: S, sample chamber; I, insulator; M, rhenium gasket; D1, upper diamond; D1, lower diamond.

pressures above 50 GPa. We performed *in situ* pressure determination using the ruby method. Several small ruby chips on the sample are irradiated by an argon laser and the empirical relation between the observed wavelength of the ruby fluorescence line and the pressure value is employed at room temperature as well as at low temperatures below 10 K.

2.3. Mbar experiments

The shape of the anvil surface was one of the most important parts of designing the DAC. A pair of 1/3 carat diamond anvils was routinely used for the high-pressure experiments. We usually ordered the diamonds with a seven-degree bevelled design of a top surface diameter of 50 or 100 μm and a culet of 300 μm. Essential for performing electrical resistance measurements at megabar pressures was the method of covering (insulating) the metal gasket. Figure 2 shows the arrangement of the megabar gasket and electrodes that we used for detecting the metallization and superconducting transition in oxygen [3], and the standard procedure is as follows.

The rhenium gasket was pre-indented to 50 μm in thickness and a thin part of the indentation was removed. Aluminium oxide (Al_2O_3) powder was placed on the pressure surface and pressed up to approximately 30 GPa or more, then a sample hole of 50 μm in diameter was made at the very centre of the gasket. Four electrodes made of 5 μm-thick platinum foil were cut in a suitable shape and pressed onto the aluminium oxide layer. We checked the insulation between the electrodes and the gasket during compression to Megabar pressures as well as during all the cooling processes. The electrical resistance was measured using a conventional four-terminal method with a dc or ac measuring current. A small ac current was better for minimizing heating of the sample during low-temperature experiments.

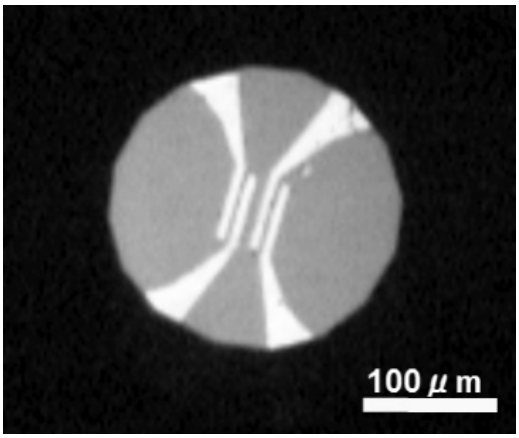

Figure 3. Deposited Cu electrodes on the culet surface of a diamond anvil for a four-probe electrical resistance measurement.

Manual setting of the four metal electrodes needs skill, and the difficulty increases towards higher pressure, where the diameter of the pressure surface becomes less than 30 μm.

To improve the situation, we used electrical circuits drawn by a lithographic technique. Figure 3 shows a photograph of the surface of the sputtered diamond anvil. In the case of using sputtered electrode, the electrodes were connected to the conventional platinum electrodes on the outside of the top face of the diamond anvil. The 'sputtered anvil' could be used only once at Megabar pressures, but it may be used many times at low pressures below 20 GPa.

The pressure is usually measured using ruby fluorescence, however at pressures of around 100 GPa the intensity of the R-line decreases and becomes comparable to the luminescence of the diamond anvil, making it difficult or impossible to determine the pressure value. The increase of the luminescence cannot be avoided, but it can be minimized by the selection of high-purity diamond.

Recently, new synthetic diamonds (type IIa) of high purity and high quality have become available. The crystal imperfections can be checked by, for example, x-ray topography. The optical properties and mechanical hardness of a high-purity synthetic diamond were much improved in Raman and infrared spectroscopy of hydrogen at Megabar pressures.

2.4. Quasi-hydrostatic experiments

In the conventional configuration described above, where the Pt electrodes are set on the pressure surface of diamond anvils, the sample was pressed directly with the diamond surface and consequently an axial stress was applied. To improve the pressure quality, an appropriate pressure medium such as helium, mixed alcohol or NaCl should be used. Figure 4 shows the arrangement of the insulator gasket; the present method for a quasi-hydrostatic pressure is as follows. The sample was cut into a shape appropriate for the scale of the chamber using a grinding machine with a thin diamond saw. Gold wires of 10 μm in diameter were bonded to the sample using a micro-manipulating electric-discharge technique [4, 5]. Then four electrodes made from platinum film were placed on the gasket close to the sample chamber and the other end of the gold wire was connected to the platinum electrodes. The sample and some small ruby chips were clamped with fluid as a pressure medium. Applying pressure up to several gigapascals, the diameter of the sample chamber was decreased slightly. NaCl was found to

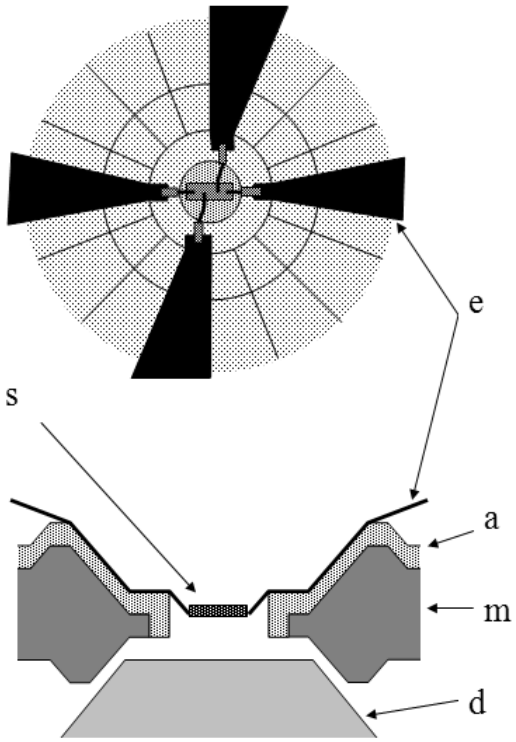

Figure 4. Arrangement of sample and electrodes for performing in quasi-hydrostatic pressure conditions in the DAC: s, sample; e, Pt film electrode (5 μm^t); a, aluminium oxide insulator; m, metal gasket; d, diamond.

be an acceptable pressure-transmitting media at pressures above 10 GPa. Figure 5 shows a photograph of the sample chamber in the DAC at a pressure of 8 GPa. This method is now mainly applied for research into pressure-induced superconductivity in heavy fermion systems which are sensitive to axial pressure and shear stress.

3. Magnetization measurements

Magnetization measurements were performed using a dc-SQUID (superconducting quantum interference detector) magnetometer with a pair of pick-up coils. Several turns of pick-up coil for the SQUID magnetometer were wound closely around the pressure surface of the diamond, with equal turns near the diamond for background compensation. A small tin chip was put inside the compensation coil as a reference sample to check the signal from the iron in both sense and magnitude. This method was available at temperatures below several kelvin, where the pick-up coil (superconducting wire such as NbTi) is in a superconducting state. Even using the sensitive coil system with a SQUID magnetometer, it was difficult to detect a relatively small signal such as that from an antiferromagnetic transition. We usually performed the magnetization measurements in order to confirm that the transition was a superconducting one, after we detected a resistance drop using the resistance measurement.

4. Examples of pressure-induced superconductivity

Here we review recent results on two pressure-induced superconductors: the cases of the elements iron and lithium.

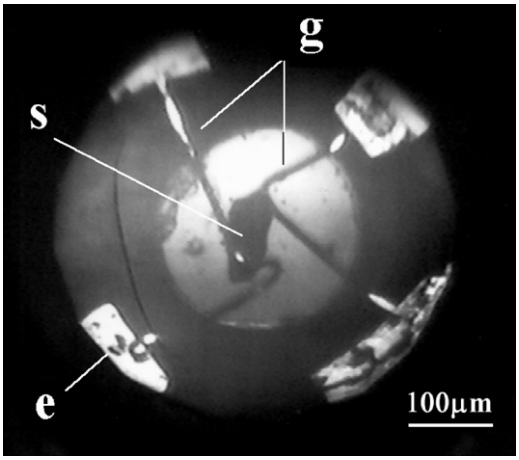

Figure 5. Photograph of sample chamber in the DAC at a pressure of 8 GPa: s, sample; g, gold wire; e, Pt film electrode.

4.1. Iron

It is well known that a ferromagnetic metal does not show superconductivity down to the lowest temperature, and even a small amount of ferro- or para-magnetic impurities could suppress the superconducting transition temperature, T_c. This is because of the pair-breaking magnetic interaction between Cooper pairs and the local magnetic moment. In contrast, we may expect the appearance of superconductivity in magnetic metals in their nonmagnetic state under a certain pressure and at low temperature. For example, iron (α Fe) is known to become a nonmagnetic metal after the crystal phase transition from the bcc (α Fe) phase to the hcp (ϵ Fe) phase under a pressure exceeding 15 GPa. In addition, there exist theories predicting a T_c of 0.25 K for ϵ Fe [6] and 2 K for hypothetical sc-Fe [7]. Recently, Suzuki *et al* performed the first-principles band calculation and predicted a pressure dependence of T_c of ϵ Fe [8].

We had searched for superconductivity in iron under pressure for several years. After searching over a wide range of pressure up to 100 GPa and temperature down to 50 mK, we noticed that purification of the sample and the application of quasi-hydrostatic pressure using an appropriate pressure medium should be most important. According to the Mössbauer-effect experiment, hcp iron shows no magnetism down to 30 mK [9]. Nasu [10] showed that the phase transition from the α phase to the ϵ phase is found to take place most successfully under hydrostatic pressure, and the amount of the remaining magnetic α Fe in the ϵ phase is pressure independent, and could be reduced down to below the resolution of the Mössbauer experiment. In fact, pressurization of the sample in a pressure medium such as NaCl was found to be very effective in the present case of iron, avoiding excess crystal distortion and uniaxial pressure distribution in the course of pressurization.

4.2. Experimental and results in Fe

An iron sample with a purity of 99.995% supplied from Johnson Matthey was purified further and degasified by heating to close to the melting point in the ultrahigh-vacuum chamber [11]. Major impurities in the starting material were O, Ta, Si and Co, with proportions of 115, 10, 8.3 and 8.3 ppm respectively, according to the chemical analysis data. The sample was cut into a rectangular shape of 0.04 (thickness) $\times$ 0.160 (length) $\times$ 0.07 (width) mm^3. Four

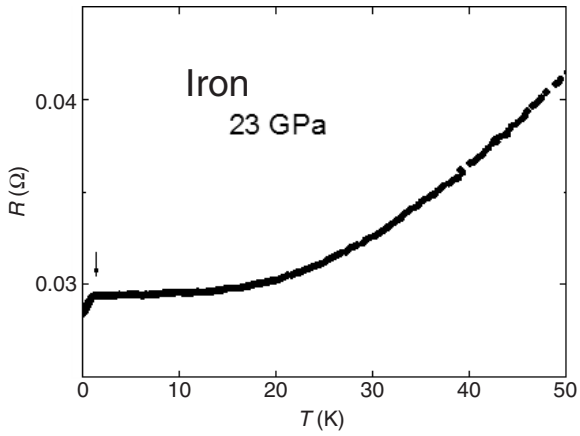

Figure 6. Obtained R–T curve below 50–30 mK at 23 GPa. A drop (arrow) indicates the onset of superconductivity at around 2 K. The residual resistance at the lowest temperature includes contributions from the gold wire in series with the sample as well as a contact resistance between the sample and the wire.

gold wires for resistance probes were welded onto the sample using the micro-spot welding technique. For electrical resistivity measurements, we performed ac four-terminal resistance measurements with a typical measuring current of 0.1×10^{-3} A at low temperatures below 10 K. The sodium chloride (NaCl) was filled into the sample chamber as the pressure-transmitting medium (figure 4) to preserve quasi-hydrostatic conditions. Several ruby chips of a size less than 0.002 mm in diameter were placed around the sample and used for pressure determination through a standard ruby fluorescence method. Pressure was applied at room temperature and the DAC was assembled on the mixing chamber ofthe ^{3}He/^{4}He dilution refrigerator.

A small but definite drop in electrical resistivity was observed at temperatures below 2 K at pressures above 16 GPa. A typical R–T curve at a pressure of 23 GPa is shown in figure 6. The drop in the resistance due to the superconducting transition was very small (less than 10% of the total residual resistance). The residual resistance included the contribution of contact resistance between the gold wire and the sample, as well as the contribution of the finite contact resistance, which is estimated to be about 90% of the measured resistance. As is expected for a conventional superconductor, the drop was suppressed and broadened with a large measuring current. Applying an external magnetic field, the resistivity drop shifted towards lower temperature and disappeared above 0.2 T. The observed measuring current as well as magnetic field dependence shows that the drop was due to the superconducting transition of iron. The measured superconducting critical field of iron was almost ten times larger than that of the superconductors rhenium or thallium. The superconductivity of ϵ Fe was also confirmed by magnetization measurements.

We studied the pressure dependence of T_c and found that T_c appears at 15 GPa and disappears at 30 GPa, giving a maximum value of 2 K at 21 GPa. We tried to estimate the phase boundary of bcc-to-hcp (α to ϵ), even if the transition under pressure is sluggish and has a wide pressure width. To determine the boundary at low temperature, the resistance was measured as a function of pressure at fixed temperature of 10 and 290 K using the same arrangement as that with which the superconductivity of iron was observed. The resistance curves showed a broad jump at the structural boundary and at 290 K; the coexistence of α and ϵ phases was 13–17 and 5–10 GPa in the course of increasing and decreasing the pressure, respectively. In the course of increasing the pressure at 10 K, a clear step in resistance was not observed, but the coexistence

was 5–10 GPa in the course of decreasing the pressure. The structural transition α to ϵ could not be detected clearly from the present electrical resistance measurements. We need further and precise investigations of the magnetic properties of the boundary region.

Recently, complete zero resistance in the superconducting transition and a nearly ferromagnetic character of the normal state has been reported [12]. Superconductivity of iron seems to appear in the nonmagnetic state, however a theoretical calculation [13] suggested that spin fluctuation coupling, especially of antiferromagnetic nature, is sufficiently large to explain the superconductivity of hcp iron. Moreover, superconductivity in the nearly (ferro) magnetic elementary metals has recently been predicted [14]. We can expect superconductivity analogously in the case of ferromagnetic cobalt and nickel as well as antiferromagnetic manganese and chromium.

4.3. Lithium

Lithium is the third element in the periodic table of elements and is well known as the lightest metal. For a long time, mono-valent metals like alkaline metals are believed not to show superconductivity even at very low temperature. However, Cs metal was found to become superconducting under pressure [15] and the possibility of pressure-induced superconductivity also arose in other lighter alkaline metals. Even so, the principal motivating force for searching for superconductivity in lithium is the possibility of a very high T_c. Recent calculations [16] predicted the pressure dependence of the T_c of lithium and gave very high T_c values, reaching up to 80 K at around 40 GPa. We also expected that highly compressed lithium can be treated as a prototype of metallic hydrogen, which is the lightest element, and was predicted to show the highest superconducting transition at near room temperature in its possible metallic state at pressures above 400 GPa [1]. Neaton and Ashcroft [17] predicted the high-pressure structure of Li at around 100 GPa as a paired state with $Cmca$ structure, similarly to dense hydrogen. The theoretical suggestion is of interest not only for finding a new crystal structure but thanks to the picture of the same scenario in metallic hydrogen and its high-T_c superconducting transition. The investigation of highly compressed low-Z elements provided a wealth of information on the fundamental properties of condensed phases of elements. In particular, their high Debye temperatures may cause a high-temperature superconducting transition, according to conventional theory.

4.4. Experimental results and results in Li

Alkaline metals are all very reactive elements, and Li especially has been known to react chemically with the diamond used in high-pressure equipment, often breaking the anvils. This high chemical activity seems to be the reason why only a small number of reports at high pressure have been presented. We searched for superconductivity in lithium using electrical resistance measurements under pressure. The sample was cut into a suitable size from high-purity ribbon (99.999%) obtained from Johnson–Matthey and loaded into a DAC. However, as mentioned, there were difficulties in confining the Li sample in the DAC because of the high activity even with diamonds as well as the gasket materials. We have tried a number of experiments and failed to keep the sample at high pressure above 30 GPa, which is caused by leakage through the spaces between the gasket and the diamond anvil. To preventing the leakage of the Li sample, we made a small pit on the insulating layer (Al_2O_3) of the gasket as well as on the surface of diamond anvil, as shown in figure 7. The 'pit-anvil' was prepared by a focused, pulsed KrF-excimer laser beam with an ultraviolet wavelength of 248 nm. We put the sample into the pit and placed the measuring electrodes of thin platinum films into the

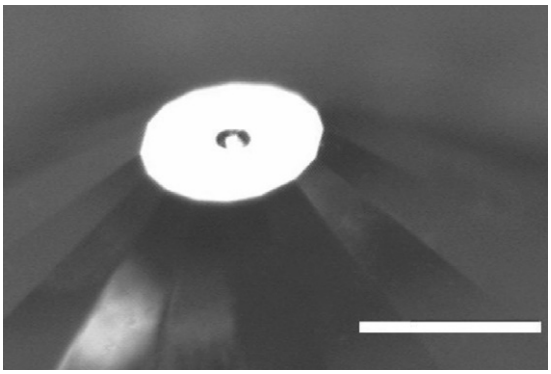

Figure 7. Photograph of a 'pit-anvil' with a pit of 50 μm in diameter and 7 μm in depth on the 300 μm pressure surface of a synthetic Ib diamond-anvil; scale bar = 0.5 mm.

pit, touching the sample. Some part of the sample spreads out from the pit at the beginning of compression, but no further leakage was observed. This procedure worked well at low temperatures and succeeded in confining the lithium samples at high pressures up to 85 GPa. All of these treatments of the sample were made in an argon atmosphere in a water- and oxygen-free glove-box. We applied pressure not exceeding 10 GPa at room temperature, and then the pressure cell was connected to the cryostat. Once the DAC cooled, pressure was applied only at temperatures lower than 50 K in order to minimize the chemical reactions. The pressure inside the DAC was applied through helium gas pressure, controlled from outside the cryostat and measured using a conventional ruby-fluorescence method through the optical windows of the cryostat.

The resistance versus temperature curves were obtained at fixed pressures. The total resistance as well as the residual resistance at low temperature increased with compression. This may show an increase in the electron–phonon coupling for instance, however some of this may include experimental uncertainty such as thinning and contamination of the sample. At pressures of 3.5 and 23 GPa, the measured resistance showed a normal metallic behaviour, however a drop in the resistance was observed at around 13 K above 35 GPa. The onset temperature of the drop slightly shifted to higher temperature at 36 GPa. We prepared another sample (in run 2) which reached up to 48 GPa, and the onset of the drop in resistance shifted higher and reached 20 K at 48 GPa. A loss in resistance exceeding 50% suggested that the drop was caused by a superconducting transition. The magnetic field dependence of the resistance drop indicated strong evidence of a superconducting transition; the drop shifted to lower temperature on applying the field and was fully suppressed above 3 T. Then we conclude that the drop was from the onset of superconductivity of Li. Observation of the Meissner signal is indispensable for the proof of superconductivity, however we had experimental difficulties in performing magnetic measurements using the gas-controlled DAC in the cryostat and did not obtain any signal. After releasing the pressure back to near atmospheric pressure at low temperature, the sample showed its original reflection of light, which indicated that no chemical reaction in the sample occurred during the experimental process. Lin and Dunn [18] had already reported the high-pressure and low-temperature electrical resistance of Li. They showed a sudden drop in resistance around 7 K, suggesting a phase transition and possibly the onset of superconductivity. The present transition showed a clear difference in the pressure dependence; their results showed no pressure dependence in the observed drop, where ours showed a significant dependence.

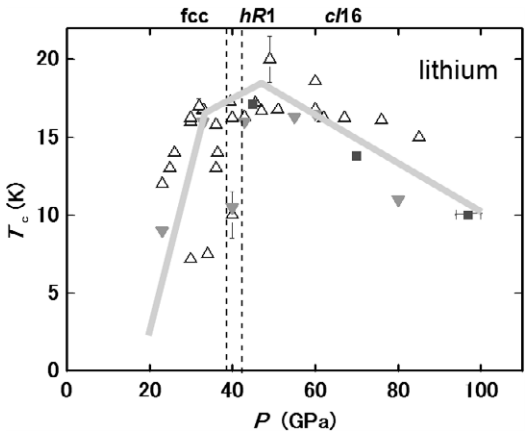

Figure 8. Pressure dependence of T_c of lithium. Dotted lines indicate the structural phase boundary observed by x-ray diffraction studies at a temperature of 180 K.

We summarize that Li undergoes a superconducting transition under pressures of more than 25 GPa, having a critical temperature of around 20 K at 48 GPa, which is the highest value ever observed in any element in the periodic table. The superconductivity appeared in a wide pressure region from fcc phase through $cI16$-phase [19]. As shown in figure 8, the curve of T_c versus pressure becomes almost flat above 40 GPa and changes in slope at around 60 GPa. The superconductivity has been confirmed experimentally by several groups [20, 21], however the pressure dependence of T_c was slightly different from figure 8. The pressure dependence of T_c may reflect the structural changes under pressure. Low-temperature investigation of the structure is needed, which may clarify the exact structure of Li in the high-T_c superconducting phase. Theoretical calculations of the superconductivity in the fcc phase have been performed recently [22, 23] and shown that the calculated values of T_c are in good agreement with our experiments.

We did not observe any sign of the metal-to-insulator transition that was predicted at pressures exceeding 100 GPa. Further experimental investigation of the higher-pressure behaviour in Li should help the total understanding of the fundamental properties of metals and possible room-temperature superconductivity in metallic hydrogen.

5. Summary

Here we have reviewed recent developments of the complex, extreme conditions of low temperature and high pressure and the results of pressure-induced superconductivity. Following these results, in future, new types of superconductivity may be discovered in elemental materials at high pressure. Our final target is, indeed, the production of metallic hydrogen and the detection of its possible high-T_c superconducting state, which is expected to be realized under the ultrahigh but almost attainable pressure of 400 GPa. We are sure that the present technique can be applied to the discovery of other superconductors, not only in simple systems but in compounds such as correlated electron systems at high pressures.

Acknowledgments

The author expresses much thanks to professors K Amaya and T C Kobayashi for critical discussions, professor M Ishizuka for his collaboration on magnetization measurements and

professor S Endo for his helpful technical support. Special thanks are due to professor Y Ōnuki for providing us with the purified Fe samples and to Dr M I Eremets for his valuable suggestions on high-pressure techniques.

References

[1] Richardson C F and Ashcroft N W 1997 *Phys. Rev. Lett.* **78** 118
[2] Wohlfarth E P 1979 *Phys. Lett.* A **75** 141
[3] Shimizu K *et al* 1998 *Nature* **393** 767
[4] Walker I R and Moss C J 1998 *Rev. Sci. Instrum.* **69** 2747
[5] Hiraoka T 1998 *Rev. Sci. Instrum.* **69** 2808
[6] Wohlfarth E P 1979 *Phys. Lett.* A **75** 141
[7] Freeman A J, Continenza A, Massida S and Grossman J C 1990 *Physica* C **166** 317
[8] Suzuki N, Souraku T and Hamada I 2001 *Proc. EHPRG '39 (Santander, 2001)*
[9] Taylor R D, Pasternak M and Jeanloz R 1991 *J. Appl. Phys.* **69** 6126
[10] Nasu S *et al* 2002 *J. Phys.: Condens. Matter* **14** 11167
[11] Haga Y *et al* 1998 *Japan. J. Appl. Phys.* **37** 3604
[12] Jaccard D, Holmes A T, Behr G, Inada Y and Onuki Y 2002 *Phys. Lett.* A **299** 282
[13] Jarlborg T 2002 *Phys. Lett.* A **300** 518
[14] Jarlborg T 2003 *Physica* C **385** 513
[15] Wittig J 1968 *Phys. Rev. Lett.* **21** 1250
[16] Christensen N E and Novikov D L 2001 *Phys. Rev. Lett.* **86** 1861
[17] Neaton J B and Ashcroft N W 1999 *Nature* **400** 141
[18] Lin T H and Dunn K J 1986 *Phys. Rev.* B **33** 807
[19] Hanfland M, Syassen K, Christensen N E and Novikov D L 2000 *Nature* **408** 174
[20] Struzhkin V V, Eremets M I, Gan W, Mao H K and Hemley R J 2002 *Science* **298** 1213
[21] Deemyad S and Schilling J S 2003 *Phys. Rev. Lett.* **91** 167001
[22] Uma Maheswari S, Nagara H, Kusakabe K and Suzuki N 2005 *J. Phys. Soc. Japan* **74** 3227
[23] Tse J S, Ma Y and Tutuncu H M 2005 *J. Phys.: Condens. Matter* **17** S911–20